Competitive Electron Transfer and Enhanced Intersystem Crossing in Photoexcited Covalent TEMPO−Perylene−3,4:9,10−bis(dicarboximide) Dyads: Unusual Spin Polarization Resulting from...

ARTICLE *in* THE JOURNAL OF PHYSICAL CHEMISTRY A · FEBRUARY 2010

Impact Factor: 2.69 · DOI: 10.1021/jp909212c · Source: PubMed

6 AUTHORS, INCLUDING:

Boiko Cohen
University of Castilla-La Mancha
63 PUBLICATIONS **2,292** CITATIONS
SEE PROFILE

Amy M Scott
Columbia University
19 PUBLICATIONS **550** CITATIONS
SEE PROFILE

Competitive Electron Transfer and Enhanced Intersystem Crossing in Photoexcited Covalent TEMPO−Perylene-3,4:9,10-bis(dicarboximide) Dyads: Unusual Spin Polarization Resulting from the Radical−Triplet Interaction

Michael T. Colvin, Emilie M. Giacobbe, Boiko Cohen, Tomoaki Miura, Amy M. Scott, and Michael R. Wasielewski*

Department of Chemistry and Argonne-Northwestern Solar Energy Research (ANSER) Center, Northwestern University, Evanston, Illinois 60208-3113

Received: September 24, 2009; Revised Manuscript Received: December 16, 2009

A stable 2,2,6,6-tetramethyl-1-piperidinyloxyl (TEMPO) radical was covalently attached at its 4-position to the imide nitrogen atom of a perylene-3,4:9,10-bis(dicarboximide) (PDI) to produce TEMPO−PDI, **1**, having a well-defined distance and orientation between TEMPO and PDI. Transient optical absorption experiments in toluene following selective photoexcitation of the PDI chromophore in TEMPO−PDI show that enhanced intersystem crossing occurs with $\tau = 45 \pm 1$ ps, resulting in formation of TEMPO−^{3*}PDI, while the same experiment in THF shows that the electron-transfer reaction TEMPO−^{1*}PDI → TEMPO$^{+\bullet}$−PDI$^{-\bullet}$ occurs with $\tau = 1.2 \pm 0.2$ ps and thus competes effectively with enhanced intersystem crossing. Time-resolved EPR (TREPR) spectroscopy on the photogenerated three-spin system TEMPO−^{3*}PDI in toluene at 295 K initially shows a broad signal assigned to spin-polarized ^{3*}PDI, which thermalizes at longer times and is accompanied by formation of an emissively polarized TEMPO radical. No signals are observed in THF at 295 K. The TREPR spectrum of TEMPO−^{3*}PDI at 85 K in toluene shows an emissive/absorptive signal due to TEMPO and a broad triplet signal due to ^{3*}PDI having a spin polarization pattern characteristic of overpopulation of its T_0 sublevel. This unusual spin polarization pattern does not result from radical pair intersystem crossing because electron transfer does not occur at 85 K. The observed spin polarization of ^{3*}PDI cannot be readily explained by mechanisms discussed previously, leading us to propose a new spin polarization mechanism, which requires that the radical and attached triplet are in the weak exchange regime.

Introduction

Photoexcitation of organic molecules can produce well-defined initial spin states,[1−6] while modern electron paramagnetic resonance (EPR) techniques provide an important means of examining these states with a view toward molecule-based spintronics.[7−11] For example, spin-selective intersystem crossing following photoexcitation often produces highly spin-polarized triplet states.[12] The interaction of these triplet states with stable radicals may result in electron spin polarization of the radical, providing a facile means for introducing and controlling spin polarization in organic materials.[13−20] A second strategy uses photoinitiated ultrafast electron transfer within covalently linked organic donor−acceptor molecules having specific donor−acceptor distances and orientations to produce highly spin-polarized radical pairs (RPs) in which the initial spin state is well defined.[21−25] We and others have investigated how to control the spin dynamics of these covalent RPs using the influence of additional spins.[26−33]

Stable free radicals are well known to quench excited states in a wide variety of noncovalent and flexibly linked covalent systems.[34−46] However, there are very few examples of rigid systems in which the structural and electronic basis of the quenching has been studied, and for the most part only fluorescence quantum yields and lifetimes have been examined.[29,47−49] Several photophysical mechanisms have been proposed to account for this quenching:[33,35,36,41,42,45,46,50]

$$^{1*}\mathrm{PDI} + {}^{2}\mathrm{R}^{\bullet} \xrightarrow{k_{ET}} {}^{2*}\mathrm{PDI}^{-\bullet} + \mathrm{R}^{+} \quad \text{(A)}$$

$$^{1*}\mathrm{PDI} + {}^{2}\mathrm{R}^{\bullet} \xrightarrow{k_{EnT}} {}^{1}\mathrm{PDI} + {}^{2*}\mathrm{R}^{\bullet} \quad \text{(B)}$$

$$^{1*}\mathrm{PDI} + {}^{2}\mathrm{R}^{\bullet} \xrightarrow{k_{EISC}} {}^{3*}\mathrm{PDI} + {}^{2}\mathrm{R}^{\bullet} \quad \text{(C)}$$

$$^{1*}\mathrm{PDI} + {}^{2}\mathrm{R}^{\bullet} \xrightarrow{k_{EIC}} {}^{1}\mathrm{PDI} + {}^{2}\mathrm{R}^{\bullet} \quad \text{(D)}$$

where A is electron transfer, B is Förster and/or Dexter energy transfer, C is electron exchange-induced enhanced intersystem crossing (EISC), and D is enhanced internal conversion (EIC), i.e., rapid vibrational relaxation. For example, electron transfer from a TEMPO free radical to the triplet state of a covalently linked 1,8:4,5-naphthalene-bis(dicarboximide) (NI) chromophore has been reported to occur with $\tau_{cs} < 15$ ns in acetonitrile, resulting in a long-lived charge-separated state with a lifetime of >200 μs.[51] In addition, several studies have reported the oxidation of nitroxide radicals by fullerene triplet states, but they are limited to intermolecular interactions.[52−54] Fluorescence quenching as a result of electron transfer to or from a stable radical has often been considered unlikely due to the lack of a solvent dependence, which is often key evidence for assigning this mechanism.[40] However, it

* To whom correspondence should be addressed. E-mail: m-wasielewski@northwestern.edu.

10.1021/jp909212c
Published on Web 01/07/2010

has been argued that a lack of solvent dependence is not definitive evidence for ruling out electron transfer, since the process could be diffusion controlled and not appear solvent dependent.[38] To date there is no conclusive evidence that the excited singlet state of a chromophore is quenched by electron transfer to or from a stable radical.

Spin polarization as a result of triplet−radical interactions has been known for several decades. Historically, spin polarization resulting from these interactions has been attributed to two mechanisms, the radical−triplet pair mechanism (RTPM)[16,20,47,55−65] and electron spin polarization transfer (ESPT).[14,57,66] In the RTPM triplet and radical diffuse toward each other and their spin states mix via the spin−spin exchange interaction (J) to produce excited doublet and quartet states. The decay rate of the excited doublet state to the ground state is more rapid than that of the excited quartet state due to conservation of spin multiplicity. The polarization (enhanced absorption or emission) is determined by the sign of J. On the other hand, an initially polarized triplet state is required for ESPT, where the polarization is transferred from the triplet to the radical by spin exchange, resulting in quenching of the triplet state to the ground-state singlet, with the polarization of the triplet determining the polarization of the radical.

Several examples of photoexcited triplet states having covalently attached radicals have appeared in the literature, e.g., ZnTPP ligated with pyridylnitronylnitroxides,[16,20,47] silicon phthalocyanines, fullerenes with 2,2,6,6-tetramethylpiperidine-*N*-oxyl (TEMPO) derivatives attached,[18,19,48,67−70] and verdazyl and nitronylnitroxides attached to polycyclic aromatic molecules.[71−75] In a few of these systems[16,18,20] excited doublet and quartet states are observed that exhibit polarization inversion (emission → absorption and vice versa) over time, which cannot be explained by RTPM or ESPT. Recently, a third mechanism, the reversed quartet mechanism (RQM),[18] was proposed to explain these results. The presence of excited doublet and quartet states results from having a fixed distance (and thus a fixed exchange interaction) between the triplet and the radical. According to the RQM, spin polarization derives from reversible transitions from the doublet manifold to the quartet manifold due to mixing by the zero-field splitting interaction. Selective depletion of the excited doublet state to the ground state leads to reversed transitions from the quartet to the doublet states, resulting in polarization inversion.

Recently, we prepared and studied a series of perylene-3,4:9,10-bis(dicarboximide) (PDI) molecules covalently attached at fixed distances to *tert*-butylphenylnitroxide radicals.[49] Upon photoexcitation, EISC from ^{1*}PDI to ^{3*}PDI occurs on a picosecond time scale. Unlike previously studied radical−triplet systems, the ultrafast formation of ^{3*}PDI is due exclusively to the presence of a stable free radical and not spin−orbit-induced intersystem crossing (SO-ISC), which is exceptionally inefficient for PDI.[76] Thus, if a stable radical is covalently linked to PDI at a fixed distance and ^{3*}PDI is formed by the interaction of ^{1*}PDI with the stable radical, the dynamics of this process can be attributed exclusively to mechanisms other than SO-ISC and thus provides an important probe of how ^{3*}PDI formation depends on the structure and electronic properties of the PDI−radical system. The spin−spin exchange interaction between ^{3*}PDI and the *tert*-butylphenylnitroxide radical initially produces spin-polarized excited doublet and quartet states followed by a polarized ground-state radical. The TREPR transitions for these states are well-resolved spectroscopically at W band (94 GHz) and indicate that polarization inversion occurs on the microsecond time scale, which is consistent with the RQM. In this paper, we present transient optical absorption and TREPR data on a stable TEMPO free radical covalently bound to PDI, **1** (TEMPO−PDI). Selective photoexcitation of the PDI chromophore in TEMPO−PDI results in solvent polarity-dependent competition between EISC leading to TEMPO−^{3*}PDI and electron transfer from TEMPO to ^{1*}PDI yielding TEMPO^{+}−PDI$^{-\bullet}$, thus providing the first direct evidence of excited singlet-state quenching leading to ion pair formation. We used TREPR to examine the interaction between ^{3*}PDI and TEMPO in **1** at both 295 and 85 K. We observe spin dynamics that cannot be readily explained by previously proposed mechanisms, leading us to propose a new mechanism of spin polarization derived from the radical−triplet interaction.

Experimental Section

Synthesis. The synthesis of **1** is described in the Supporting Information.

Optical Spectroscopy. Ground-state absorption measurements were made on a Shimadzu (UV-1601) spectrophotometer. The optical density of all samples was maintained between 0.3 and 0.6 at 532 nm ($\varepsilon_{\mathrm{PDI,\ 532\ nm}} = 30\,500\ \mathrm{cm^{-1}\ M^{-1}}$)[24] for both femtosecond and nanosecond transient absorption spectroscopy. Femtosecond transient absorption measurements were made using the 532 nm, 130 fs output from an optical parametric amplifier using techniques described earlier.[77] Samples were placed in a 2 mm path length glass cuvette and bubbled with nitrogen to prevent sample degradation. The samples were irradiated with 0.5−1.0 μJ per pulse focused to a 200 μm spot. The total instrument response function (IRF) for the pump−probe experiments was 180 fs. Samples for nanosecond transient absorption spectroscopy were placed in a 10 mm path length quartz cuvette equipped with a vacuum adapter and subjected to five freeze−pump−thaw degassing cycles. The samples were excited with 6 ns, 1 mJ, 545 nm laser pulses generated using the frequency-tripled output of a Continuum 8000 Nd:YAG laser to pump a Continuum Panther OPO. The excitation pulse was focused to a 5 mm diameter spot and matched to the diameter of the probe pulse generated using a xenon flashlamp (EG&G Electro-Optics FX-200). The signal was detected using a photomultiplier tube with high voltage applied to only 4 dynodes (Hamamatsu R928). The total instrument response time is 7 ns and determined primarily by the laser pulse duration. Transient absorption kinetics were fit to a sum of exponentials with a Gaussian instrument function using Levenberg−Marquardt least-squares fitting.

EPR Spectroscopy. EPR measurements at both X band (9.5 GHz) and W band (94 GHz) were made using a Bruker Elexsys E680-X/W EPR spectrometer outfitted with a variable Q dielectric resonator (ER-4118X-MD5-W1) at X band and a cylindrical resonator (EN-680-1021H) at W band. For EPR measurements at X band, toluene solutions of **1** ($\sim 10^{-4}$ M) were loaded into quartz tubes (4 mm o.d. × 2 mm i.d.), subjected to five freeze−pump−thaw degassing cycles on a vacuum line (10^{-4} mBar), and sealed using a hydrogen torch. For EPR measurements at W band, samples of **1** ($\sim 10^{-4}$ M) were loaded into quartz tubes (0.84 mm o.d. × 0.6 mm i.d.) in a N_2-filled glovebox to a height of ~8 mm and sealed with a clear ridged UV doming epoxy (Epoxies, Etc., DC-7160 UV). The EPR samples were stored in a freezer in the dark when not being used.

Steady-state CW EPR spectra were measured at X band using 0.2−2 mW microwave power and 0.01−0.05 mT field modulation at 100 kHz. The temperature was controlled by an Oxford Instruments CF935 continuous flow cryostat using liquid N_2. TREPR measurements were made using continuous wave (CW)

microwaves at 295 K with direct detection and field swept electron spin echo (ESE) detection at 85 K, where the echo intensity was integrated as the field was swept. The samples were photoexcited at 532 nm (0.2 mJ/pulse, 7 ns, 10 Hz) using the frequency-doubled output from a Nd:YAG laser (Quanta-Ray DCR-2). For W-band experiments, laser light was coupled to a fiber optic sample holder (Bruker E-600-1023 L). For room-temperature measurements, kinetic traces of the transient magnetization were accumulated under CW microwave irradiation (2−20 mW) after photoexcitation. The field modulation was disabled to achieve a $Q/\pi\nu \approx 30$ ns instrument response function (IRF), where Q is the quality factor of the resonator and ν is the resonant frequency, while microwave signals in emission (e) and/or enhanced absorption (a) were detected in both the real and the imaginary channels (quadrature detection). Sweeping the magnetic field gave 2D spectra versus both time and magnetic field. For each kinetic trace, the signal acquired prior to the laser pulse was subtracted from the data. Kinetic traces recorded at magnetic field values off resonance were considered background signals, whose average was subtracted from all kinetic traces. For pulsed experiments at X band, a 1 kW TWT amplifier (Applied Systems Engineering 117X) was employed to generate high-power microwave pulses. The resonator was fully decoupled for pulsed experiments ($Q < 200$). ESE data was obtained with a $\pi/2-\tau-\pi$ pulse sequence with $\pi/2 = 8$ ns, $\pi = 16$ ns, and $\tau = 140$ ns. After the transient species is generated by the laser pulse, the integrated echo intensity is recorded as a function of the magnetic field to yield the spectrum at a given time after the laser pulse. For both detection methods the spectra were phased into a Lorentzian part and a dispersive part, and the former, also known as the imaginary magnetic susceptibility χ, is presented.

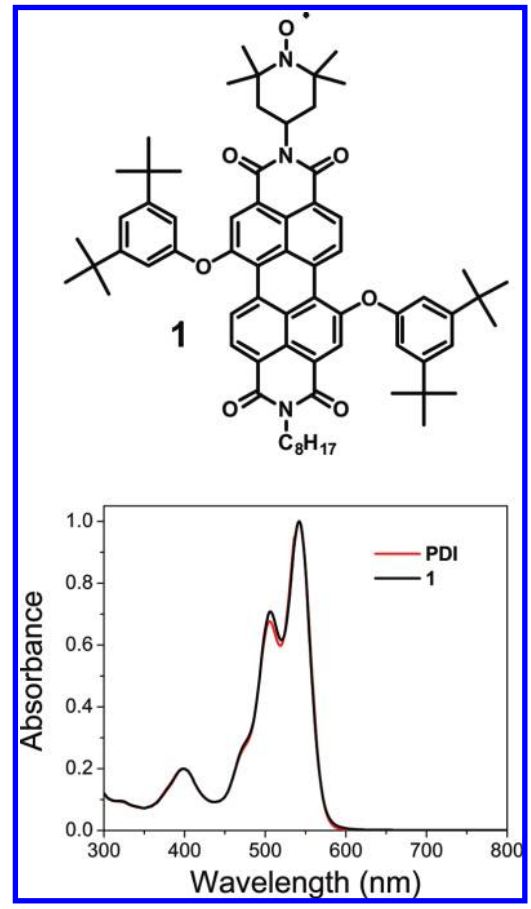

Figure 1. UV−vis spectra of **1** and *N,N*-dioctyl-PDI in toluene.

Results

Synthesis and Steady-State Characterization. The synthesis of **1** is described in detail in the Supporting Information. Briefly *N*-(2-ethylhexyl)-1,7-(3′,5′-di-*tert*-butylphenoxy)perylene-3,4-dicarboxyanhydride-9,10-dicarboximide anhydride (PIA) was refluxed with 4-amino-TEMPO in pyridine for 12 h to yield **1**, which was purified by silica gel column chromatography using 2% acetone in dichloromethane as the eluent. Compound **1** was further purified by preparative TLC immediately prior to use. Figure 1 shows the UV−vis absorption spectra of **1** and *N,N*-dioctyl-PDI in toluene. PDI has a strong absorption at 545 nm ($\varepsilon = 46\,000$ M^{-1} cm^{-1}),[78] which does not change significantly upon attachment to TEMPO, indicating that the electronic coupling between PDI and TEMPO is relatively weak. The absorption feature between 300 and 350 nm is due to TEMPO. The PDI chromophore is normally highly fluorescent ($\Phi_F = 0.98$);[76] however, the fluorescence of **1** is strongly quenched ($\phi_F < 0.001$) in both toluene and THF.

Transient Absorption Spectroscopy. The transient absorption spectra of **1** in toluene (Figure 2) reveals that ^{1*}PDI decays with $\tau = 45 \pm 1$ ps when probed at 720 nm, where ^{1*}PDI absorbs. Another broad feature appears between 430 and 500 nm with $\tau = 43 \pm 1$ ps, which has been previously attributed to the formation of ^{3*}PDI,[79] and the rise time matches the decay of ^{1*}PDI within experimental uncertainty. The transient absorption changes of ^{3*}PDI extend well into the microsecond time scale, but the intrinsic ^{3*}PDI lifetime was not obtained due to diffusion-limited triplet−triplet annihilation (Figure 3). In contrast, the transient absorption spectroscopy of **1** in THF is quite different. The near-infrared transient absorption band at 725 nm sharpens rapidly with $\tau = 1.2 \pm 0.2$ ps, indicative of the formation of $PDI^{\bullet-}$.[80] The $TEMPO^{+}-PDI^{\bullet-}$ charge-separated state decays to $\Delta A = 0$ with $\tau = 86 \pm 1$ ps, and no residual signal due to ^{3*}PDI is observed.

EPR Spectroscopy. Steady-state (CW) and TREPR spectra are shown in Figure 4. The CW spectrum of **1** ($g = 2.0057$, $a_N = 1.5$ mT) has three lines resulting from coupling of the electron spin to a single ^{14}N. No other hyperfine couplings are observed, indicating that the electron spin density is localized on the N−O group. The intensity of the hyperfine lines decreases with M_I, indicative of a slower rotational correlation time (fast motion limit)[81] due to the TEMPO radical being attached to a larger molecule (PDI). Initially, the TREPR spectrum of **1** following selective photoexcitation of PDI with a 532 nm laser pulse (Figure 4b) consists of a broad (10 mT, peak to peak) feature with an emissive signal at lower field and an absorptive signal at higher field, which decays with $\tau = 109 \pm 6$ ns and has a absorptive feature that lasts into the microsecond time scale (Figure S2, Supporting Information). At later times (Figure 4c), the spectrum appears very different, consisting of a broad absorptive feature (fwhm = 8.0 mT) and three spin-polarized signals (1.5 mT splitting) having enhanced *emission*. Both signals decay on a microsecond time scale. To aid in our assignments, a TREPR spectrum was acquired at W band (94 GHz) (Figure S3, Supporting Information). At short times, the spectrum looks similar to that obtained at X band, while the broad absorptive feature and polarized hyperfine lines are absent at longer times. The measured g value of the transient is 2.0032.

The TREPR spectrum at 85 K (Figure 5) shows a broad spectrum with an *a,e,e,a,a,e* spin polarization pattern and an emissive/absorptive feature in the middle at $g \approx 2$. We confirmed the phase of the pattern by recording a properly phased field swept electron spin echo (ESE) detected spectrum

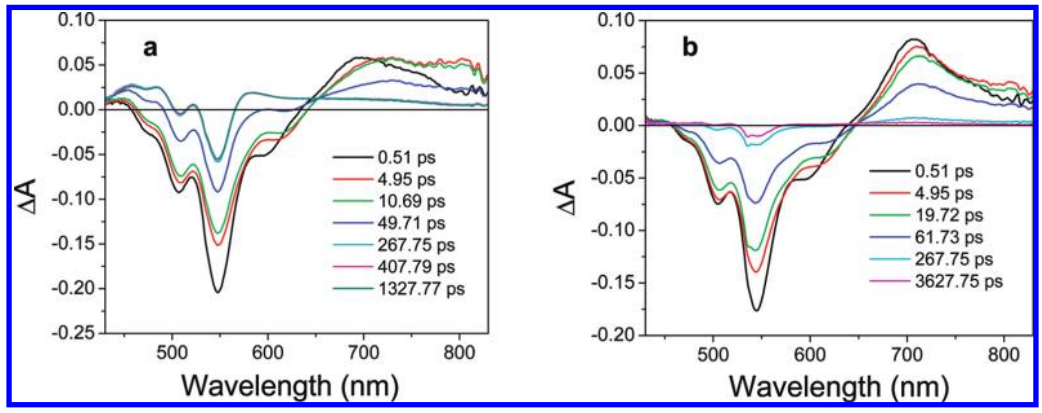

Figure 2. Transient absorption spectra of **1** in (a) toluene and (b) THF at the times indicated.

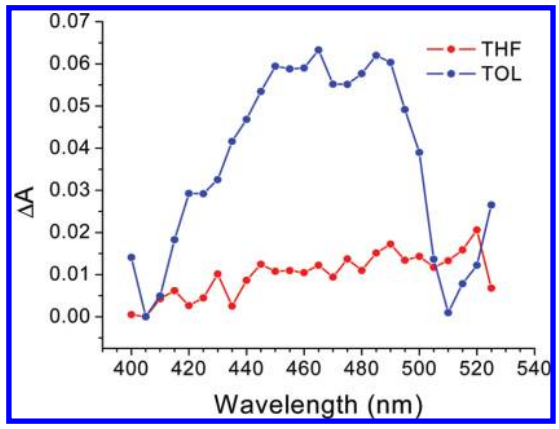

Figure 3. Nanosecond transient absorption of **1** in toluene and THF obtained with samples having the same ground-state absorbance at the excitation wavelength.

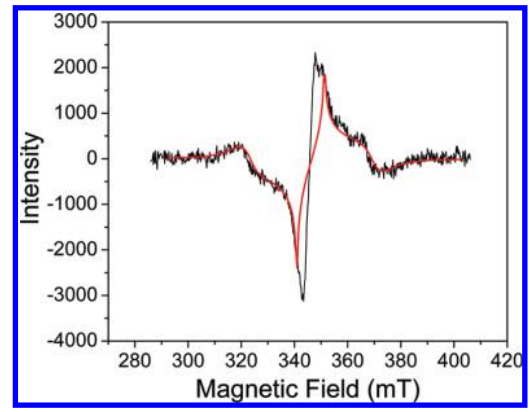

Figure 5. TREPR spectrum of **1**, along with its simulation (in red) in toluene at 85 K, 1 μs after the laser pulse. The central signal is due to spin-polarized TEMPO.

of the radical in the dark and subtracting it from the photoexcited spectrum. Assuming that the broad feature is ^{3*}PDI, simulation of the spectrum yields zero-field splitting parameters $D = 28$ mT and $E = -6$ mT. The D value is somewhat smaller than that observed previously for ^{3*}PDI ($D = 40$ mT), while the E value is similar.[22,82,83] The emissive signal in the center of the spectrum is the TEMPO radical. All spectral features decay on the microsecond time scale. The *a,e,e,a,a,e* spin polarization pattern of ^{3*}PDI results from overpopulation of the T_0 sublevel and has been observed previously only in systems in which radical pairs are formed and undergo radical pair intersystem crossing (RP-ISC) followed by charge recombination to the local triplet state.[22,83,84] However, RP-ISC is not a viable pathway in **1** because (1) we do not observe electron transfer from TEMPO to PDI in toluene at both 295 and 85 K and (2) RP-ISC requires

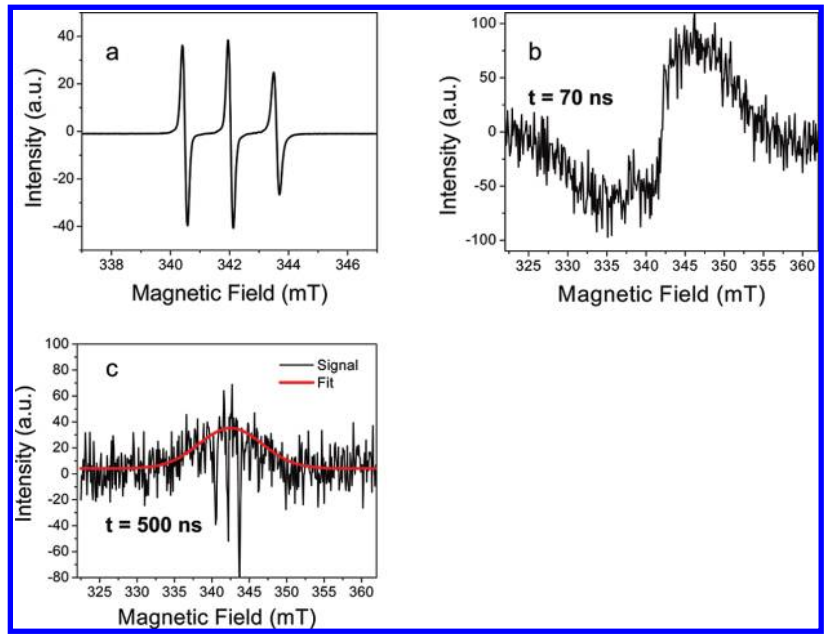

Figure 4. EPR spectra of **1** at 295 K: (a) CW EPR spectrum and (b and c) TREPR spectra following a 7 ns, 532 nm laser flash.

two unpaired spins so that even if electron transfer did occur in our system there would only be one unpaired spin.

Discussion

Electron Transfer vs EISC. The femtosecond transient absorption spectra and kinetics of **1** show that ^{1*}PDI decays rapidly in the presence of TEMPO in both toluene ($\tau = 45 \pm 1$ ps) and THF ($\tau = 1.2 \pm 0.2$ ps) compared to its intrinsic 4.5 ns lifetime.[76] However, it appears that the quenching mechanism changes as a function of solvent. In toluene we observe ^{3*}PDI formation, while in THF we observe PDI$^{\bullet-}$. The formation of PDI$^{\bullet-}$ in THF indicates that the electron-transfer reaction TEMPO−^{1*}PDI → TEMPO^{+}−PDI$^{-\bullet}$ is responsible for quenching the singlet state, providing the first direct evidence of singlet-state quenching due to electron transfer. The free energies of reaction for TEMPO−^{1*}PDI → TEMPO^{+}−PDI$^{-\bullet}$ are $\Delta G_{CS} = -0.31$ in toluene and −0.83 in THF (Supporting Information). The magnitude of ΔG_{CS} indicates that the electron-transfer reaction is in the normal region of the Marcus rate versus free energy dependence,[85] so that charge separation should be faster in THF than in toluene. Since EISC should not be solvent dependent and EISC occurs with $\tau = 45$ ps in toluene, if there are no other competitive processes the quantum yield of electron transfer in THF is 0.97.

The ultrafast formation of ^{3*}PDI from ^{1*}PDI in toluene is most likely due to the EISC mechanism.[50] The electron exchange interaction between ^{1*}PDI and TEMPO serves as the first-order perturbation that drives EISC.[49] The magnitude of this perturbation, and thus the overall intersystem crossing rate, depend strongly on the electronic overlap between the orbitals that contribute to ^{1*}PDI and the singly occupied molecular orbital (SOMO) of TEMPO and the energy gap between ^{1*}PDI and ^{3*}PDI. Since the energy gap between these two states is about 1.2 eV,[79] one might expect that EISC would be slower than observed. However, semiempirical ZINDO/S calculations[86] place the T_2 state of PDI (^{3**}PDI) nearly isoenergetic with ^{1*}PDI. This makes it more likely that EISC occurs between ^{1*}PDI and ^{3**}PDI, followed by very rapid internal conversion from ^{3**}PDI to ^{3*}PDI.

Radical−Triplet Interactions and Time-Resolved EPR Spectroscopy. The spin Hamiltonian for radical−triplet interactions is given as

$$\hat{H} = \hat{H}_Z + \hat{H}_{hf} + \hat{H}_{Dip} + \hat{H}_{Ex} = g_T\beta_e B\hat{S}_Z^T + g_R\beta_e B\hat{S}_Z^R + \sum_i \hat{S}^R\mathbf{A}\mathbf{I}_i + \hat{S}^T D_T \hat{S}^T + \hat{S}^T D_{TR}\hat{S}^R + J_{TR}\hat{S}^T\hat{S}^R \quad (1)$$

where β_e is the Bohr magneton, g_T and g_R are the g values for the triplet and ground-state radical, respectively, B is the magnetic field, $\mathbf{A}$ is the hyperfine tensor and becomes a, the isotropic hyperfine coupling constant, in fluid solution, $\hat{S}$ and I are the electron and nuclear spin operators, D is the dipolar interaction, and J is the exchange interaction.

When the exchange interaction between the electron on the radical and the electrons on the triplet, $|J_{TR}|$, is larger than the other magnetic interactions (strong exchange regime), the exchange interaction removes the spin degeneracy resulting in the formation of excited doublet and quartet states.[87] Conversely, when $|J_{TR}|$ is smaller than the other magnetic interactions (weak exchange regime) the excited doublet and quartet states are not good quantum states and should display transitions similar to those of the ground-state doublet and lowest triplet states.[87] In the strong exchange regime the g values of the excited doublet (g_D) and quartet (g_Q) should be linear combinations of the ground-state doublet (g_R) and excited triplet (g_T), according to eqs 2 and 3,[87] while the hyperfine coupling constants a_N should follow eqs 4 and 5. The zero-field splitting parameters for a quartet are different from a triplet and obey eq 6, where D_Q is the zero field splitting of the quartet, D_T is the zero-field splitting of the triplet, and D_{TR} is the dipole−dipole interaction between the electrons on the triplet and the electron on the radical. In the weak exchange limit the EPR spectrum should show separate resonances for the triplet and ground-state radical with the corresponding hyperfine splittings and g values.

$$g_D = -\frac{1}{3}g_R + \frac{4}{3}g_T \quad (2)$$

$$g_Q = \frac{1}{3}g_R + \frac{2}{3}g_T \quad (3)$$

$$a_N^D = -\frac{1}{3}a_N^R \quad (4)$$

$$a_N^Q = \frac{1}{3}a_N^R \quad (5)$$

$$D_Q = \frac{1}{3}(D_T + D_{TR}) \quad (6)$$

Unlike other covalently bound radical−triplet systems that have been examined,[16,18,20,49] we do not observe polarization inversion for **1**. Furthermore, the spectra are broad compared to those observed in our previous work.[49] The three spin-polarized signals present at the center of the TREPR spectrum in Figure 4c, which are separated by 1.5 mT, are assigned to ground-state TEMPO since the observed hyperfine splitting matches that of the CW EPR spectrum of **1**. The presence of excited doublet and quartet states in **1** is unlikely since eqs 4 and 5 predict that their hyperfine splittings should be 0.5 mT. We previously measured the g value of the excited doublet state in *tert*-butylphenylnitroxides attached to ^{3*}PDI to be 2.0025 and that of the quartet state to be 2.0040.[49] These values should be the same for **1** because ^{3*}PDI is the same and the g values of TEMPO and *tert*-butylphenylnitroxide are identical. Using these g values and $g = 2.0057$ for the TEMPO ground state, eqs 2 and 3 predict that $g = 2.0033$ for ^{3*}PDI, which matches the g value we measured at W band within experimental uncertainty. On the basis of these results, we assign the signal present at 70 ns to ^{3*}PDI (Figure 4b). The presence of the ^{3*}PDI triplet in **1** is confirmed by the broad spectrum observed at 85 K (Figure 5). The D value obtained from the simulation (28 mT) is smaller than that previously reported for ^{3*}PDI (∼40 mT)[22] but larger than the ∼12 mT zero-field splitting predicted by eq 6 for a pure quartet state (the D_{TR} calculation is given in the Supporting Information). The D value of ^{3*}PDI in our system is smaller compared to previous systems,[22,82,83] while the E value remains similar. This discrepancy may be due to the dipolar and/or exchange interaction between the triplet and the radical, neither of which is accounted for in our simulation. The TREPR spectrum of the quartet state has been observed when a *tert*-butylphenylnitroxide is attached to ^{3*}PDI and is substantially narrower than that of ^{3*}PDI.[49] The narrowing of the quartet-state signal relative to that of the triplet state

of a given chromophore is consistent with literature reports.[47,88] We employ a triplet simulation that accounts for anisotropic broadening but is not an ideal simulation for our system if J_{TR} is large enough to add some quartet character to the observed signal. Mixing quartet character into the triplet may result in reduction of the observed D value. While these data support our assertion that the radical−triplet interaction within **1** is in the weak exchange regime, it also suggests that this is a borderline case.

In the past decade the triplet states of C_{60},[89,90] porphyrins,[20,91] phthalocyanines,[91,92] and subphthalocyanines[91,93] have been observed in isotropic media as broad featureless signals. The TREPR signals for the triplet states of porphyrins, phthalocyanines, and subphthalocyanines decay biexponentially with the short component attributed to spin relaxation of the spin-polarized triplet and the long component attributed to population decay of the thermalized triplet. Molecule **1** also has a short emissive component and a diffusion-limited absorptive component (Figure S2, Supporting Information). With this in mind, we assign the spectrum shown in Figure 4b to spin-polarized ^{3*}PDI and the broad signal shown in Figure 4c to thermalized ^{3*}PDI.

Our results are inconsistent with the current mechanisms used to explain CIDEP induced by radical−triplet interactions. The RTPM requires diffusive encounters to mix the high-field triplet eigenstates T_{+1}, T_0, and T_{-1} with the α and β spin states of the radical to produce the excited doublet and quartet manifolds. Since **1** has a fixed triplet−radical distance, the RTPM is not applicable, while ESPT results in quenching of the triplet, which is not observed. The observations of the polarized ground-state radical and a triplet state, as opposed to excited doublet and quartet states, and the lack of polarization inversion implies that the RQM is also not responsible for our observations. As a result, we propose a new mechanism to explain our results. We believe that these results can be rationalized by assuming that the exchange interaction between the radical and the triplet is smaller than the other magnetic interactions (weak exchange regime). In the weak exchange regime we should observe a ground-state radical and a triplet state with their individual g values and hyperfine coupling constants.[87] The polarization inversion observed in RQM is due to reversible transitions between the excited doublet and quartet states and selective depletion of the excited doublet to the ground state.[18,49] Since our system does not possess fully developed excited doublet and quartet states, we do not have reversible transitions and therefore do not observe polarization inversion. Generation of ^{3*}PDI by EISC indicates a nonzero exchange interaction between the singlet excited state and the radical, while the interaction between the triplet state and the radical appears to be small. Theoretical[94] and experimental[95] studies suggest that the long-range exchange interaction is governed by perturbations from coherent charge-transfer interactions involving virtual CT states. In toluene, the energy gap between the CT state and the singlet excited state is 0.31 eV, which is three times smaller than the energy gap between the triplet state and the CT state (0.89 eV). This difference may reconcile the efficient EISC with the very small triplet−radical interaction.

However, the EISC rate observed in **1** is significantly slower compared to our previously studied PDI covalently attached to *tert*-butylphenylnitroxide system (∼2 ps), which shows a very strong triplet−radical interaction.[49] This indicates relatively weak electronic coupling in **1,** probably due to localized unpaired electron density on the N−O group of TEMPO, whereas in our previously studied system the SOMO of the *tert*-butylphenylnitroxide radical has spin density delocalized on to the phenyl ring, which increases the electronic coupling.

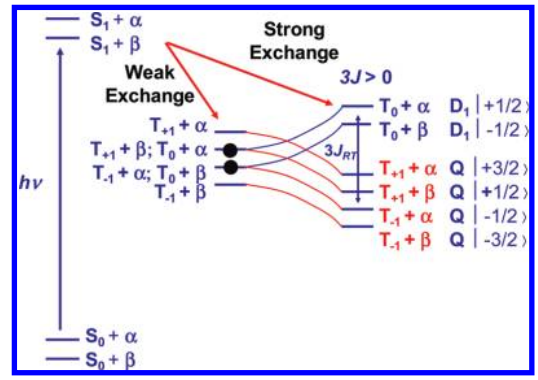

Figure 6. Energy levels for **1** in the weak and strong exchange regimes.

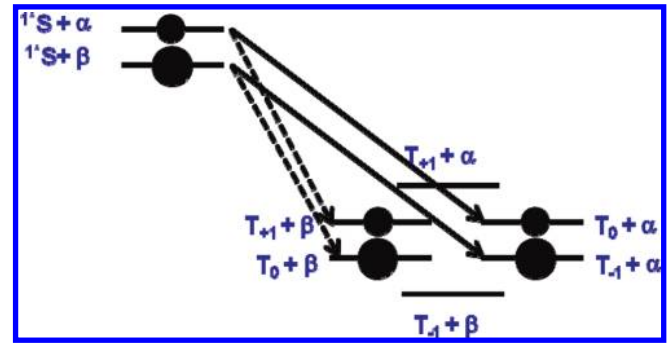

Figure 7. Schematic of EISC to different sublevels, where M_s is conserved.

The observations that the ground-state radical is polarized in emission (Figure 4c) and that ^{3*}PDI has the *a*,*e*,*e*,*a*,*a*,*e* spin polarization pattern, indicative of overpopulation of the T_0 sublevel,[22] (Figure 5) need to be explained by any proposed mechanism. To date, the only observations of this polarization pattern have been for triplet states generated by charge recombination following RP-ISC. In fact, this polarization pattern has been the unique signature of the RP-ISC mechanism. The observed polarization of **1** can be explained by selective population of the energy levels shown in Figure 6. Since spin−orbit coupling is negligible in PDI and the exchange interaction is isotropic, EISC in our system is unlikely to depend on molecular symmetry. EISC has also been examined theoretically, where it was found that the isotropic exchange interaction is solely responsible for ISC in systems where spin−orbit coupling is negligible, as is the case for **1**, where M_s is conserved.[94,96] Conservation of M_s in **1** results in the two central sublevels being populated (Figure 6). Initially the radical possesses thermal polarization, which should not change upon excitation to the first excited state of PDI. EISC from ^{1*}PDI−TEMPO to ^{3*}PDI−TEMPO then occurs and according to theory should conserve M_s.[94,96] This selection rule allows for the population of the 4 center states shown in Figure 7. The conservation of M_s can occur by two pathways: in the first M_s of the ^{3*}PDI remain the same ($^{1*}S-T_0$ transition) and the α or β state of the radical remain constant, while the second changes the M_s of ^{3*}PDI ($^{1*}S-T_{\pm1}$ transition) and is compensated for by the change in the α or β state of the radical. If the second pathway does not occur then the polarization should match thermal equilibrium, in which case no transient polarization change should be observed. In contrast, if the second pathway occurs to any extent then the α sublevel should have more population than it does at thermal equilibrium, resulting in

negative transient signal, namely, canceling of the positive thermal polarization. In the limit where the second pathway occurs exclusively the transient signal should be negative with twice the intensity as thermal polarization (details are given in the Supporting Information).

The simulation indicates that the central radical signal appears to possess an emission/absorption (E/A) type polarization at low temperature. This may result from the dipolar interaction between the radical and the triplet, which shift the energies of the six radical−triplet states so that three radical transitions do not cancel each other out in a manner similar to spin-correlated radical pair spectra.[97,98] This effect is insignificant at room temperature due to the fast tumbling of the molecule, which averages out the dipolar interaction.

The question arises as to why our system has weak exchange, as only one other such system, a [70]fulleropyrrolidine nitroxide, has been reported to date,[70] while other closely related systems[16,18,20,49] are in the strong exchange regime. Exchange interactions require either direct overlap of the relevant orbitals or a superexchange interaction involving virtual orbitals in the molecular framework connecting the sites of high spin density, both of which should be relatively small in our system. First, the TEMPO radical is localized because its σ-bond system insulates its spin density from that on ^{3*}PDI minimizing J. Second, there is no direct overlap between the N−O group of the TEMPO radical and the π system of PDI, which should also minimize J. The other system reported in the weak exchange regime also has characteristics similar to those of **1**, i.e., a localized radical constrained to a geometry that keeps it apart from the triplet chromophore.[70]

Lastly, we address the apparent contradiction of accelerated EISC from ^{1*}PDI to ^{3*}PDI but slow intersystem crossing from ^{3*}PDI to ground-state PDI. As mentioned previously, since exchange-induced intersystem crossing is driven by a first-order perturbation, it should depend on the energy gap, so that the observed fast intersystem crossing is a result of transitions from ^{1*}PDI to ^{3**}PDI (small energy gap) followed by fast relaxation from ^{3**}PDI to ^{3*}PDI. Since the energy gap from ^{3*}PDI to the PDI ground state is 1.2 eV, the exchange-induced intersystem crossing should be slower because the energy gap is large. Furthermore, transitions between ^{3*}PDI and the PDI ground state are restricted to formally spin forbidden intersystem crossing as the only viable pathway, unlike systems in the strong exchange regime where spin-allowed internal conversion is also viable pathway.

Conclusions

Our results show that TEMPO quenches ^{1*}PDI by EISC in toluene and by electron transfer in THF. This is the first direct evidence of quenching of an excited singlet-state chromophore as a result of electron transfer involving a radical. Unlike previously studied systems, the electron spin polarization observed following rapid EISC results in formation of a triplet state weakly exchange coupled to a ground-state radical. To account for the observed TREPR spectra, we propose a spin polarization mechanism in which the radical and triplet are in the weak exchange regime, with the T_0 sublevel overpopulated, where the emissive radical signal results from the nearly equal initial population of the radical α and β states.

Acknowledgment. This work was supported by the National Science Foundation under grant no. CHE-0718928 and the MRSEC program of the NSF through the Northwestern MRSEC (DMR-0520513). The authors thank Ms. Charusheela Ramanan, Dr. Qixi Mi, and Dr. Raanan Carmieli for their assistance and useful discussions. M.T.C. thanks the Link Foundation for a fellowship.

Supporting Information Available: Experimental details, including synthesis, additional transient absorption, and TREPR data. This material is available free of charge via the Internet at http://pubs.acs.org.

References and Notes

(1) Wasielewski, M. R. *J. Org. Chem.* **2006**, *71*, 5051.
(2) Verhoeven, J. W. *J. Photochem. Photobiol. C* **2006**, *7*, 40.
(3) Segura, J. L.; Martin, N.; Guldi, D. M. *Chem. Soc. Rev.* **2005**, *34*, 31.
(4) Holten, D.; Bocian, D. F.; Lindsey, J. S. *Acc. Chem. Res.* **2002**, *35*, 57.
(5) Lukas, A. S.; Wasielewski, M. R. Approaches to a Molecular Switch using Photoinduced Electron and Energy Transfer. In *Molecular Switches*; Feringa, B. L., Ed.; Wiley-VCH: Weinheim, 2001; p 1.
(6) de Silva, A. P.; Guanaratne, H. Q. N.; Gunnlaugsson, T.; Huxley, A. J. M.; McCoy, C. P.; Rademacher, J. T.; Rice, T. E. *Chem. Rev.* **1997**, *97*, 1515.
(7) Rajca, A. *Adv. Phys. Org. Chem.* **2005**, *40*, 153.
(8) Mehring, M.; Mende, J. *Phys. Rev. A: At. Mol. Opt. Phys.* **2006**, *73*, 052303/1.
(9) Harneit, W. *Phys. Rev. A* **2002**, *65*, 032322.
(10) Jones, J. A. Experiments leading toward quantum computation: Nuclear magnetic resonance experiments. In *The physics of quantum information*; Bouwmeester, D., Ekert, A., Zeilinger, A., Eds.; Springer: Berlin, 2000; p 177.
(11) Schweiger, A.; Jeschke, G. *Principles of pulsed electron paramagnetic resonance*; Oxford: Oxford, 2001.
(12) Levanon, H.; Norris, J. R. *Chem. Rev.* **1978**, *78*, 185.
(13) Blank, A.; Levanon, H. *J. Phys. Chem. A* **2000**, *104*, 794.
(14) Blank, A.; Levanon, H. *J. Phys. Chem. A* **2001**, *105*, 4799.
(15) Franco, L.; Mazzoni, M.; Corvaja, C.; Gubskaya, V. P.; Berezhnaya, L. S.; Nuretdinov, I. A. *Mol. Phys.* **2006**, *104*, 1543.
(16) Fujisawa, J.; Ishii, K.; Ohba, Y.; Yamauchi, S.; Fuhs, M.; Möbius, K. *J. Phys. Chem. A* **1999**, *103*, 213.
(17) Kawai, A.; Shibuya, K. *J. Photochem. Photobiol., C* **2006**, *7*, 89.
(18) Rozenshtein, V.; Berg, A.; Stavitski, E.; Levanon, H.; Franco, L.; Corvaja, C. *J. Phys. Chem. A* **2005**, *109*, 11144.
(19) Sartori, E.; Toffoletti, A.; Corvaja, C.; Garlaschelli, L. *J. Phys. Chem. A* **2001**, *105*, 10776.
(20) Fujisawa, J.; Ishii, K.; Ohba, Y.; Yamauchi, S.; Fuhs, M.; Möbius, K. *J. Phys. Chem. A* **1997**, *101*, 5869.
(21) Carbonera, D.; Di Valentin, M.; Corvaja, C.; Agostini, G.; Giacometti, G.; Liddell, P. A.; Kuciauskas, D.; Moore, A. L.; Moore, T. A.; Gust, D. *J. Am. Chem. Soc.* **1998**, *120*, 4398.
(22) Dance, Z. E. X.; Mi, Q.; McCamant, D. W.; Ahrens, M. J.; Ratner, M. A.; Wasielewski, M. R. *J. Phys. Chem. B* **2006**, *110*, 25163.
(23) Hasharoni, K.; Levanon, H.; Greenfield, S. R.; Gosztola, D. J.; Svec, W. A.; Wasielewski, M. R. *J. Am. Chem. Soc.* **1995**, *117*, 8055.
(24) Weiss, E. A.; Ahrens, M. J.; Sinks, L. E.; Gusev, A. V.; Ratner, M. A.; Wasielewski, M. R. *J. Am. Chem. Soc.* **2004**, *126*, 5577.
(25) Weiss, E. A.; Ratner, M. A.; Wasielewski, M. R. *J. Phys. Chem. A* **2003**, *107*, 3639.
(26) Chernick, E. T.; Mi, Q.; Vega, A. M.; Lockard, J. V.; Ratner, M. A.; Wasielewski, M. R. *J. Phys. Chem. B* **2007**, *111*, 6728.
(27) Mi, Q.; Chernick, E. T.; McCamant, D. W.; Weiss, E. A.; Ratner, M. A.; Wasielewski, M. R. *J. Phys. Chem. A* **2006**, *110*, 7323.
(28) Chernick, E. T.; Mi, Q.; Kelley, R. F.; Weiss, E. A.; Jones, B. A.; Marks, T. J.; Ratner, M. A.; Wasielewski, M. R. *J. Am. Chem. Soc.* **2006**, *128*, 4356.
(29) Ishii, K.; Hirose, Y.; Kobayashi, N. *J. Phys. Chem. A* **1999**, *103*, 1986.
(30) Mori, Y.; Sakaguchi, Y.; Hayashi, H. *J.Phys.Chem.A* **2000**, *104*, 4896.
(31) Mori, Y.; Sakaguchi, Y.; Hayashi, H. *Bull. Chem. Soc. Jpn.* **2001**, *74*, 293.
(32) Vlassiouk, I.; Smirnov, S.; Kutzki, O.; Wedel, M.; Montforts, F.-P. *J. Phys. Chem. B* **2002**, *1−6*, 8657.
(33) Buchachenko, A. L.; Berdinsky, V. L. *Chem. Rev.* **2002**, *102*, 603.
(34) Hrdlovic, P.; Chmela, S.; Sarakha, M.; Lacoste, J. *J. Photochem. Photobiol., A* **2001**, *138*, 95.
(35) Karpiuk, J.; Grabowski, Z. R. *Chem. Phys. Lett.* **1989**, *160*, 451.
(36) Kollar, J.; Hrdlovic, P.; Chmela, S.; Sarakha, M.; Guyot, G. *J. Photochem. Photobiol., A* **2005**, *171*, 27.
(37) Blough, N. V.; Simpson, D. J. *J. Am. Chem. Soc.* **1988**, *110*, 1915.

(38) Chattopadhyay, S. K.; Das, P. K.; Hug, G. L. *J. Am. Chem. Soc.* **1983**, *105*, 6205.
(39) Herbelin, S. E.; Blough, N. V. *J. Phys. Chem. B* **1998**, *102*, 8170.
(40) Green, J. A.; Singer, L. A.; Parks, J. H. *J. Chem. Phys.* **1973**, *58*, 2690.
(41) Green, S. A.; Simpson, D. J.; Zhou, G.; Ho, P. S.; Blough, N. V. *J. Am. Chem. Soc.* **1990**, *112*, 7337.
(42) Kuz'min, V. A.; Tatikolov, A. S. *Chem. Phys. Lett.* **1977**, *51*, 45.
(43) Likhtenstein, G. I.; Ishii, K.; Nakatsuji, S.-i. *Photochem. Photobiol.* **2007**, *83*, 871.
(44) Medvedeva, N.; Martin, V. V.; Weis, A. L.; Likhtenshten, G. I. *J. Photochem. Photobiol., A* **2004**, *163*, 45.
(45) Sartori, E.; Toffoletti, A.; Corvaja, C.; Moroder, L.; Formaggio, F.; Toniolo, C. *Chem. Phys. Lett.* **2004**, *385*, 362.
(46) Yee, W. A.; Kuzmin, V. A.; Kliger, D. S.; Hammond, G. S.; Twarowski, A. J. *J. Am. Chem. Soc.* **1979**, *101*, 5104.
(47) Ishii, K.; Fujisawa, J.; Ohba, Y.; Yamauchi, S. *J. Am. Chem. Soc.* **1996**, *118*, 13079.
(48) Ishii, K.; Hirose, Y.; Fujitsuka, H.; Ito, O.; Kobayashi, N. *J. Am. Chem. Soc.* **2001**, *123*, 702.
(49) Giacobbe, E. M.; Mi, Q.; Colvin, M. T.; Cohen, B.; Ramanan, C.; Scott, A. M.; Yeganeh, S.; Marks, T. J.; Ratner, M. A.; Wasielewski, M. R. *J. Am. Chem. Soc.* **2009**, *131*, 3700.
(50) Hoytink, G. J. *Acc. Chem. Res.* **1969**, *2*, 114.
(51) Green, S.; Fox, M. A. *J. Phys. Chem.* **1995**, *99*, 14752.
(52) Araki, Y.; Luo, H.; Islam, S. D. M.; Ito, O.; Matsushita, M. M.; Iyoda, T. *J. Phys. Chem. A* **2003**, *107*, 2815.
(53) Borisevich, Y. E.; Kuz'min, V. A.; Renge, I. V.; Darmanyan, A. P. *Izv. Akad. Nauk SSSR, Ser. Khim.* **1981**, 2014.
(54) Samanta, A.; Kamat, P. V. *Chem. Phys. Lett.* **1992**, *199*, 635.
(55) Blättler, C.; Jent, F.; Paul, H. *Chem. Phys. Lett.* **1990**, *166*, 375.
(56) Corvaja, C.; Franco, L.; Toffoletti, A. *Appl. Magn. Reson.* **1994**, *7*, 257.
(57) Fujisawa, J.; Ishii, K.; Ohba, Y.; Iwaizumi, M.; Yamauchi, S. *J. Phys. Chem.* **1995**, *99*, 17082.
(58) Fujisawa, J.; Ohba, Y.; Yamauchi, S. *Chem. Phys. Lett.* **1998**, *282*, 181.
(59) Goudsmit, G. H.; Paul, H.; Shushin, A. I. *J. Phys. Chem.* **1993**, *97*, 13243.
(60) Hugerat, M.; van der Est, A.; Ojadi, E.; Biczok, L.; Linschitz, H.; Levanon, H.; Stehlik, D. *J. Phys. Chem.* **1996**, *100*, 495.
(61) Jenks, W. S.; Turro, N. J. *J. Am. Chem. Soc.* **1990**, *112*, 9009.
(62) Kawai, A.; Obi, K. *J. Phys. Chem.* **1992**, *96*, 52.
(63) Kawai, A.; Okutsu, T.; Obi, K. *J. Phys. Chem.* **1991**, *95*, 9130.
(64) Regev, A.; Galili, T.; Levanon, H. *J. Phys. Chem.* **1996**, *100*, 18502.
(65) Turro, N. J.; Khudyakov, I. V.; Bossmann, S. H.; Dwyer, D. W. *J. Phys. Chem.* **1993**, *97*, 1138.
(66) Fujisawa, J.; Ohba, Y.; Yamauchi, S. *J. Phys. Chem. A* **1997**, *101*, 434.
(67) Takeuchi, S.; Ishii, K.; Kobayashi, N. *J. Phys. Chem. A* **2004**, *108*, 3276.
(68) Corvaja, C.; Franco, L.; Mazzoni, M. *Appl. Magn. Reson.* **2001**, *20*, 71.
(69) Conti, F.; Corvaja, C.; Toffoletti, A.; Mizuochi, N.; Ohba, Y.; Yamauchi, S.; Maggini, M. *J. Phys. Chem. A* **2000**, *104*, 4962.
(70) Conti, F.; Corvaja, C.; Busolo, F.; Zordan, G.; Maggini, M.; Weber, S. *Phys. Chem. Chem. Phys.* **2009**, *11*, 495.
(71) Teki, Y.; Tamekuni, H.; Takeuchi, J.; Miura, Y. *Angew. Chem., Int. Ed.* **2006**, *45*, 4666.
(72) Teki, Y.; Kimura, M.; Narimatsu, S.; Ohara, K.; Mukai, K. *Bull. Chem. Soc. Jpn.* **2004**, *77*, 95.
(73) Teki, Y.; Nakatsuji, M.; Miura, Y. *Mol. Phys.* **2002**, *100*, 1385.
(74) Teki, Y.; Miyamoto, S.; Nakatsuji, M.; Miura, Y. *J. Am. Chem. Soc.* **2001**, *123*, 294.
(75) Teki, Y.; Miyamoto, S.; Iimura, K.; Nakatsuji, M.; Miura, Y. *J. Am. Chem. Soc.* **2000**, *122*, 984.
(76) Giaimo, J. M.; Lockard, J. V.; Sinks, L. E.; Scott, A. M.; Wilson, T. M.; Wasielewski, M. R. *J. Phys. Chem. A* **2008**, *112*, 2322.
(77) Ahrens, M. J.; Sinks, L. E.; Rybtchinski, B.; Liu, W. H.; Jones, B. A.; Giaimo, J. M.; Gusev, A. V.; Goshe, A. J.; Tiede, D. M.; Wasielewski, M. R. *J. Am. Chem. Soc.* **2004**, *126*, 8284.
(78) van der Boom, T.; Hayes, R. T.; Zhao, Y. Y.; Bushard, P. J.; Weiss, E. A.; Wasielewski, M. R. *J. Am. Chem. Soc.* **2002**, *124*, 9582.
(79) Ford, W. E.; Kamat, P. V. *J. Phys. Chem.* **1987**, *91*, 6373.
(80) Gosztola, D.; Niemczyk, M. P.; Svec, W.; Lukas, A. S.; Wasielewski, M. R. *J. Phys. Chem. A* **2000**, *104*, 6545.
(81) Eaton, S. S.; Eaton, G. R. *Electron Paramagn. Reson.* **2004**, *19*, 318.
(82) Carmieli, R.; Zeidan, T. A.; Kelley, R. F.; Mi, Q.; Lewis, F. D.; Wasielewski, M. R. *J. Phys. Chem. A* **2009**, *113*, 4691.
(83) Zeidan, T. A.; Carmieli, R.; Kelley, R. F.; Wilson, T. M.; Lewis, F. D.; Wasielewski, M. R. *J. Am. Chem. Soc.* **2008**, *130*, 13945.
(84) Dance, Z. E. X.; Ahrens, M. J.; Vega, A. M.; Ricks, A. B.; McCamant, D. W.; Ratner, M. A.; Wasielewski, M. R. *J. Am. Chem. Soc.* **2008**, *130*, 830.
(85) Marcus, R. A. *J. Chem. Phys.* **1956**, *24*, 966.
(86) *Hyperchem*; Hypercube Inc.: FL, 1994.
(87) Bencini, A.; Gatteschi, D. *Electron paramagnetic resonance of exchange coupled systems*; Springer-Verlag: Berlin, New York, 1990.
(88) Ishii, K.; Fujisawa, J.-i.; Adachi, A.; Yamauchi, S.; Kobayashi, N. *J. Am. Chem. Soc.* **1998**, *120*, 3152.
(89) Closs, G. L.; Forbes, M. D. E.; Piotrowiak, P. J. *J. Am. Chem. Soc.* **1992**, *114*, 3285.
(90) Levanon, H.; Regev, A.; Galili, T.; Hugerat, M.; Chang, C. K.; Fajer, J. *J. Phys. Chem.* **1993**, *97*, 13198.
(91) Yamauchi, S. *Bull. Chem. Soc. Jpn.* **2004**, *77*, 1255.
(92) Saiful, I. S. M.; Fujisawa, J.; Kobayashi, N.; Ohba, Y.; Yamauchi, S. *Bull. Chem. Soc. Jpn.* **1999**, *72*, 661.
(93) Yamauchi, S.; Takahashi, A.; Iwasaki, Y.; Unno, M.; Ohba, Y.; Higuchi, J.; Blank, A.; Levanon, H. *J. Phys. Chem. A* **2003**, *107*, 1478.
(94) Yeganeh, S.; Wasielewski, M. R.; Ratner, M. A. *J. Am. Chem. Soc.* **2009**, *131*, 2268.
(95) Kawai, A.; Shibuya, K. *J. Phys. Chem. A* **2007**, *111*, 4890.
(96) Chiu, Y.-N. *J. Chem. Phys.* **1972**, *56*, 4882.
(97) Closs, G. L.; Forbes, M. D. E.; Norris, J. R. *J. Phys. Chem.* **1987**, *91*, 3592.
(98) Buckley, C. D.; Hunter, D. A.; Hore, P. J.; McLauchlan, K. A. *Chem. Phys. Lett.* **1987**, *135*, 307.

JP909212C